Received: 10 September 2020 | Revised: 16 November 2020 | Accepted: 4 December 2020

DOI: 10.1002/cyto.a.24288

TECHNICAL NOTE

MIFlowCyt ISAC CYTOMETRY Journal of Quantitative Cell Science PART A

Development of a 43 color panel for the characterization of conventional and unconventional T-cell subsets, B cells, NK cells, monocytes, dendritic cells, and innate lymphoid cells using spectral flow cytometry

Fairooz Sahir[1] | Jericha Miles Mateo[1] | Martin Steinhoff[2,3,4,5,6,7] | Kodappully Sivaraman Siveen[1]

[1]Flow Cytometry Core Facility, Translational Research Institute, Academic Health System, Hamad Medical Corporation, Doha, Qatar

[2]Department of Dermatology and Venereology, Hamad Medical Corporation, Doha, Qatar

[3]Dermatology Institute, Hamad Medical Corporation, Doha, Qatar

[4]Translational Research Institute, Academic Health System, Hamad Medical Corporation, Doha, Qatar

[5]Department of Dermatology, Weill Cornell Medicine-Qatar, Doha, Qatar

[6]Qatar University, Medical School, Doha, Qatar

[7]Department of Medicine, Weill Cornell Medical College, New York, New York

Correspondence
Kodappully Sivaraman Siveen, Flow Cytometry Core Facility, Translational Research Institute, Academic Health System, Hamad Medical Corporation, Doha, Qatar.
Email: siveenks@me.com

Funding information
Hamad Medical Corporation, Grant/Award Numbers: MRC-03-19-039, IRGC-04-SI-17-151, IRGC-03-NI-17-071

Abstract

Although many flow cytometers can analyze 30–50 parameters, it is still challenging to develop a 40+ color panel for the phenotyping of immune cells using fluorochrome conjugated antibodies due to limitations in the availability of spectrally unique fluorochromes that can be excited by the commonly used laser lines (UV, Violet, Blue, Green/Yellow-green, and Red). Spectral flowcytometry is capable of differentiating fluorochromes with significant overlap in the emission spectra, enabling the use of spectrally similar fluorochrome pairs such as Brilliant Blue 515 and FITC in a single panel. We have developed a 43 color panel to characterize most of the immune subsets within the peripheral immune system, including conventional T cells, unconventional T cells such as invariant natural killer T cells (iNKT), Gamma delta (γδ) T-cell subsets (TCR Vδ2, TCR Vγ9) and mucosal-associated invariant T cells (MAIT), B-cell subsets, natural killer (NK) cells, plasmacytoid dendritic cells, dendritic cell subsets, hematopoietic progenitor cells, basophils, and innate lymphoid cell (ILC) subsets (CD117, CRTH2). The panel includes surface markers to analyze activation (CD38, HLA-DR, ICOS/CD278), differentiation (CD45RA, CD27, CD28, CD57), expression of cytokine and chemokine receptors (CD25, CD127, CCR10, CCR6, CCR4, CXCR3, CXCR5, CRTH2/CD294), and co-inhibitory molecules and exhaustion (PD-1, CD223/LAG-3, TIGIT), which enables a deep characterization of PBMCs from peripheral blood. Cells were analyzed on a 5-laser Cytek Aurora and data analysis was done using FlowJo. This panel can help to make a thorough interpretation of immune system, specifically when specimen quantity is low. The panel has not been completely optimized but would rather act as a guide toward the development of a workflow for optimized multicolor immunophenotyping panel.

KEYWORDS
dendritic cells, innate lymphoid cells, immunophenotyping, spectral flow cytometry, unconventional T cells

INTRODUCTION

Flow cytometry is the most frequently used high-throughput single-cells analysis technology that enables characterization of highly heterogenous samples such as blood and bone marrow. Advancements in multicolor flow cytometry and cytometry by time of flight (CyTOF) have enabled researchers to perform deep phenotyping of immune cells with sufficient sensitivity and resolution that is necessary to monitor the immune system of patients with impaired immune system such as cancer, autoimmune disorders, and so on and unravel the interaction between immune subsets. CyTOF technology have theoretical capability to detect approximately 130 isotopes, but most of the published research articles used 40–45 protein markers (maximum panel size of 47; [1]) due to limitations in the availability of isotopes and signal spillover (minimal levels compared to fluorochrome spillover) that exist between isotopes. Moreover, CyTOF has limitations such as low sample acquisition rate (around 1000 cells per second), and the destructive process prevents sorting of samples. Some of the major advantages of CyTOF are the ability to run panel with 40–45 protein markers, barcoding for multiplexing samples, and the ability to cryopreserve samples after staining. On the other hand, traditional fluorochrome-based flow cytometry is limited to 40 protein markers as per recent publications [2]. Even though there are more than 100 fluorochromes available for use in flow cytometry, most of them share same excitation and emission maximum, which limit the ability to use them in combination within a single panel. But, there are major benefits compared to CyTOF such as high event rates (up to 100,000 events per second) and the availability of instruments that allow sorting of unique target cells.

Spectral flow cytometry eliminates some of the drawbacks of traditional flow cytometry by measuring the complete emission spectrum and later unmixing the spectrum to identify individual fluorochromes. This enables the use of fluorochromes with similar excitation and emission maximum in a single panel which, in turn, increases the number of protein markers that can be analyzed. The most common examples are, the ability to use combinations such as BV421 – Pacific Blue, BV480 – SYTOX Blue, eFluor506 – BV510, Brilliant Blue 515 – FITC, PerCP – Brilliant Blue 700 – PerCP-eFluor710, CF555 – PE – CF568, PE/Dazzle594 – CF594 – PE-Alexa Fluor 610, and APC – Alexa Fluor 647 that are not possible with traditional flow cytometry. But the use of such spectrally similar fluorochrome combinations need careful panel designing and only few combinations will provide satisfactory resolution of markers.

The immunophenotyping panel presented in this study uses 42 surface markers and a viability stain to comprehensively characterize human PBMCs, covering more than 130 distinct cell populations in human peripheral blood including all major immune cell subsets and hematopoietic stem cells (HSCs), by spectral flow cytometry.

MATERIALS AND METHODS

Peripheral blood mononuclear cells (PBMCs) from healthy donor, purchased from iQBiosciences (Berkeley, CA), were used as samples. Veri-Cells PBMC (Biolegend, San Diego, CA) was used for titrations, when applicable. Stain Buffer (FBS) (BD Biosciences, San Jose, CA) was used for washing and resuspending cells, unless mentioned otherwise. AbC Total Antibody Compensation Bead Kit (Invitrogen, Waltham, MA) was used for creating fluorochrome reference controls in Cytek SpectroFlo software (Cytek Biosciences, Fremont, CA), for all the antibodies used in the study. Reference control for SYTOX Blue Dead Stain was created using PBMCs. The antibodies used in the study are listed in Table 1. Antibody master mix contained Brilliant Stain Buffer Plus (BD Biosciences) to alleviate staining artifacts. Mix-n-Stain CF Dye Antibody Labeling Kits for CF514 and CF594 were purchased from Biotium (CA) and conjugated to CRTH2 and CD1c antibodies, respectively, as per instructions from kit manufacturer. Titration experiments were carried out to determine the antibody concentration providing highest stain index. To reduce the spillover and increase resolution of markers in multicolor sample staining, most of the antibodies needed reduction in concentrations calculated based on single stains.

The study used commercially available human PBMCs (iQBiosciences). The company had lawfully obtained samples from healthy donors and it was approved by an Institutional Review Board (IRB) or Human Subject Committee. The company had obtained a signed and witnessed consent form from donor volunteers prior to starting the collection protocol.

Staining and acquisition of samples

For each staining, 1×10^6 PBMCs were used. PBMCs were thawed as per standard protocols and incubated with Human TruStain FcX Fc Receptor Blocking Solution (Biolegend) and True-Stain Monocyte Blocker (Biolegend) for 10 min. Pretitrated volumes of antibodies were prepared as a master mix and mixed with PBMCs in the wells of a Laminar Wash 96-well plate (Curiox Biosystems Co., Ltd, Seoul, South Korea). The final volume in each well was 30 µl and incubated for 40 min at room temperature in dark. Then, the cells were washed by laminar flow using the Curiox Laminar Wash System HT1000 for nine cycles. Subsequently, the cells were resuspended in stain buffer (FBS) containing SYTOX Blue Dead Cell Stain and transferred to regular 96-well U bottom plate for acquisition in Cytek Aurora flow cytometer (5-laser; 355 nm, 405 nm, 488 nm, 561 nm, and 640 nm) using the SpectroFlo Software v2.2.0.2. The cells were unmixed using the stored reference controls, with autofluorescence extraction option enabled. To reduce the unmixing errors, we had compared the spectrum of the single stain reference controls to the expected spectrum profile provided by Cytek Full Spectrum Viewer (at https://spectrum.cytekbio.com). The plots used for the gating strategy (Figure 1) did not show any significant unmixing errors. The unmixed FCS files were used for further data analysis.

Seven technical replicates (all taken from same vial of PMBC) of the sample were stained. flowAI [3] was run on all samples with default setting to check for variations in flow rate, signal acquisition, and dynamic range, and events that are marked as high quality by the

TABLE 1 List of antibodies used in the study. Cell viability was determined using SYTOX Blue Dead Cell Stain, which is also included in the list

Sl no	Excitation laser	Fluorochrome	Emission Max (nm)	Detector	Marker	Manufacturer	Cataloge no	Clone
1	355 nm	BUV395	395	UV2	CD45RA	BD	740298	HI100
2		DyLight 350	432	UV6	FcεRI	NovusBio	NBP1-43278UV	AER-37
3		BUV496	496	UV7	CD16	BD	612944	3G8
4		BUV563	563	UV9	TCR Vγ9	BD	748863	B3
5		BUV615	615	UV10	TCR Vα24-Jα18	BD	751563	6B11
6		BUV661	661	UV11	CD11c	BD	612967	B-ly6
7		BUV737	737	UV14	CD56	BD	612766	NCAM16.2
8		BUV805	805	UV16	TCR Vδ2	BD	748580	B6
9	405 nm	BV421	421	V1	PD1 (CD279)	BD	562516	EH12
10		Pacific Blue	452	V3	CD38	Biolegend	356628	HB-7
11		SYTOX Blue	480	V5	Viability	Thermo	S34857	
12		BV480	478	V5	IgD	BD	566138	IA6-2
13		eFluor506	506	V7	CD223 (LAG-3)	Thermo	69-2239-42	3DS223H
14		BV510	510	V7	CCR4	BD	563,066	1G1
15		BV570	570	V8	HLA DR	Biolegend	307638	L243
16		BV605	605	V10	CD28	BD	742527	L293
17		BV650	650	V11	CXCR3 (CD183)	BD	740603	1C6/ CXCR3
18		BV711	711	V13	CCR6 (CD196)	BD	563923	11A9
19		BV750	750	V14	CXCR5 (CD185)	BD	747111	RF8B2
20		BV786	785	V15	TIGIT	BD	747838	741,182
21	488 nm	BB515	515	B1	CCR10	BD	564769	1B5
22		FITC	520	B2	CD57	BD	555619	NK-1
23		CF514	548	B3	CRTH2 (CD294)	Biolegend	350102 (unconjugated)	BM16
24		PerCP	676	B8	CD34	Biolegend	328642	H43A
25		BB700	695	B9	TCR Vα7.2	BD	749483	OF-5A12
26		PerCP Cy5.5	695	B9	CD141	Biolegend	344112	M80
27		PerCP eFluor710	710	B10	TCR γδ	Thermo	46-9959-42	B1.1
28		BB790-P	790	B14	CD8	BD	Custom	HIT8a
29	561 nm	PE	578	YG1	ICOS (CD278)	BD	557802	DX29
30		CF568	584	YG2	CD4	Biotium	BNC680206-500	C4/206
31		PE Dazzle594	610	YG3	CD24	Biolegend	311134	ML5
32		CF594	615	YG3	CD1c	Biolegend	331502 (unconjugated)	L161
33		PE-AF 610	607	YG4	CD19-PE AF610	Thermo	MHCD1922	SJ25-C1
34		PE-Cy5	667	YG5	CD10	BD	555376	HI10a
35		PE-Cy5.5	694	YG7	CD117	NovusBio	NBP1-43358PECY55	YB5.B8
36		PE Cy7	785	YG9	CD25 (IL-2Rα)	BD	557741	M-A251
37	640 nm	APC	660	R1	CD27	BD	561400	M-T271
38		AF647	667	R2	CD161	Biolegend	339910	HP-3G10
39		Spark NIR 685	685	R3	CD14	Biolegend	367150	63D3

(Continues)

TABLE 1 (Continued)

Sl no	Excitation laser	Fluorochrome	Emission Max (nm)	Detector	Marker	Manufacturer	Cataloge no	Clone
40		APC R700	704	R4	CD127 (IL-7Rα)	BD	565185	HIL-7R-M21
41		AF700	719	R4	CD123-AF700	Biolegend	306040	6H6
42		APC-Vio770	775	R7	TCR Vβ11	Miltenyi	130-108-735	REA559
43		APCFire810	794	R8	CD3	Biolegend	344858	SK7

algorithm was used for further analysis. All FCS files were gated on single, live cells and concatenated to a single FCS file, which was used for manual gating, dimensionality reduction (UMAP and opt-SNE) and clustering (FlowSOM) analysis. For clustering and dimensionality reduction analysis all 42 surface markers were selected. UMAP [4] was run with default settings while for opt-SNE [5], Perplexity was increased to 50 to achieve optimal clustering. FlowSOM [6] was run with SOM grid size 30 × 30 and number of meta clusters 45.

Manual gating of samples

Initially, the PBMCs were identified based on the FSC and SSC parameters. Doublets were removed and single cells were selected by analyzing FSC pulse area versus width. RBCs were removed by plotting side-scatter from 488 nm laser (SSC-B) versus side-scatter from 405 nm laser (SSC). RBCs were found to have higher SSC-B along with low SSC when compared to PBMCs. Live cells were then selected using SYTOX Blue Dead Cell Stain. Monocytes were identified based on the expression of CD14 (CD14 + CD3-CD56-CD19-CD123-HLA-DR+) following the gating strategy of Shikuma et al. [7] and were subsequently divided into three subsets; classical ($CD14^{++}CD16^{-}$), intermediate ($CD14^{++/+}CD16^{+}$), and nonclassical monocytes ($CD14^{+}CD16^{++}$). T ($CD3^{+}$) and B ($CD19^{+}$) cells were gated from non-monocyte population generated by a Boolean gate.

$CD3^{+}$ T cells were analyzed to gate unconventional T-cells subsets γδ T ($TCR\gamma\delta^{+}$) cells, followed by MAIT (TCR $V\alpha7.2^{+}CD161^{+}$), iNKT (TCR $V\alpha24\text{-}J\alpha18^{+}$TCR $V\beta11^{+}$), and the remaining conventional T cells. The conventional T cells were further gated to identify $CD4^{+}$ helper, $CD8^{+}$ cytotoxic, double negative, and double positive T cells. Regulatory T cells (Tregs) were identified within the $CD4^{+}$ helper cells as $CD25^{high}CD127^{low}$ cells. Th subsets (Th_1—$CCR4^{-}CXCR3^{+}CCR10^{-}CCR6^{+}$, Th_2—$CCR4^{+}CXCR3^{-}CCR10^{-}CCR6^{-}$, Th_9—$CCR6^{+}CCR4^{-}$, Th_{17}—$CCR4^{+}CXCR3^{-}CCR10^{-}CCR6^{+}$, Th_{22}—$CCR6^{+}CCR4^{+}CCR10^{+}$, and T_{FH}—$CXCR5^{+}$) within the non-Treg CD4 cells were gated based on the expression of cytokine receptors [8]. CCR4, CXCR3, and CCR6 expression were analyzed in Tregs to identify Th-like lineages (Th_2 like – $CCR4^{+}CCR6^{-}CXCR3^{-}$, Th_{17} like – $CCR4^{+}CCR6^{+}CXCR3^{-}$, Th_1 like – $CCR4^{+}CCR6^{+}CXCR3^{-}$, and $Th_{1/17}$ like – $CCR4^{+}CCR6^{+}CXCR3^{+}$) as described by Halim et al. [9]. We have used CD45RA along with the costimulatory molecule CD27 to classify T-cell subsets (γδT cells, iNKT, MAIT, $CD4^{+}$ and $CD8^{+}$) into various differentiation stages such as naïve ($CD27^{-}CD45RA^{-}$), central memory (CM; $CD27^{+}CD45RA^{-}$), effector memory (EM; $CD27^{-}CD45RA^{-}$), and effector memory T cells that re-express CD45RA ($CD27^{-}CD45RA^{+}$; EMRA). Activation status of various T-cell subsets was monitored by evaluating the expression of CD38, HLA-DR, ICOS, CD25, and CD127. T-cell exhaustion was evaluated based on the expression of PD1 and TIGIT. T-cell senescence was determined by the upregulation of CD57 and loss of CD28.

Within the $CD19^{+}$ B cells, transitional B cells were identified as $CD10^{+}IgD^{+}CD38^{+}$ [10], plasmablast cells as $CD10^{-}CD27^{+}CD38^{+}$ and regulatory B cells as $CD10^{-}CD24^{HI}CD38^{HI}$ [11]. Expression of CD27 and IgD was used to classify $CD10^{-}$ B cells into: naïve ($IgD^{+}CD27^{-}$), switched memory B ($IgD^{-}CD27^{+}$; SM B), nonswitched memory B ($IgD^{+}CD27^{+}$; NSM B), and IgD and CD27 double negative B cells ($IgD^{-}CD27^{-}$; DN B).

Dendritic cells ($CD11c^{+}$ HLA-DR^{+}) were selected from the $CD14^{-}CD3^{-}CD19^{-}$ (nonmonocyte, T, B) cells and further gated to identify $CD141^{+}$ conventional DC1 (cDC1), $CD1c^{+}$ conventional DC2 (cDC2), $CD16^{+}$ conventional DC, and $CD141^{-}CD1c^{-}$ $CD16^{-}$ conventional DC [12]. Afterward, plasmacytoid dendritic cells (pDC; HLA-$DR^{+}CD123^{+}$) and basophils (HLA-$DR^{-}CD123^{+}Fc\varepsilon RI^{+}$) were gated from the remaining cells (nonmonocyte, T, B, DC cells), followed by NK cells, which were gated into the early NK ($CD16^{-}CD56^{++}$), mature NK ($CD16^{+}CD56^{+}$), and terminal NK ($CD16^{++}CD56^{-}$) subsets. The remaining (nonmonocyte, T, B, DC, pDC, basophil, NK) cells were gated into $CD34^{+}$ cells and $CD34^{-}Fc\varepsilon RI^{-}$ subset. The latter subset which is negative for lineage markers (CD14, CD3, CD19, CD11c, HLA-DR, CD123, CD16, CD56, CD34, and FcεRI) was used to gate $CD127^{+}$ innate lymphoid cells (ILC), which was further gated into ILC1 ($CD117^{-}$, $CRTH2^{-}$), ILC2 ($CD117^{-}$, $CRTH2^{+}$), and ILC3 ($CD117^{+}$, $CRTH2^{-}$) subsets [13]. Hematopoietic progenitor cells (HPCs) were identified as $CD34^{+}CD38^{-}$ cells.

RESULTS AND DISCUSSION

Our data demonstrate that 40+ color panels are possible with fluorochrome-based flow cytometry even though the marker and fluorochrome selection and pairing are a tedious, but feasible task. Figure 1 shows the manual gating strategy for the 43 color panel used in this study while Figure S1(A) shows most relevant fluorescence

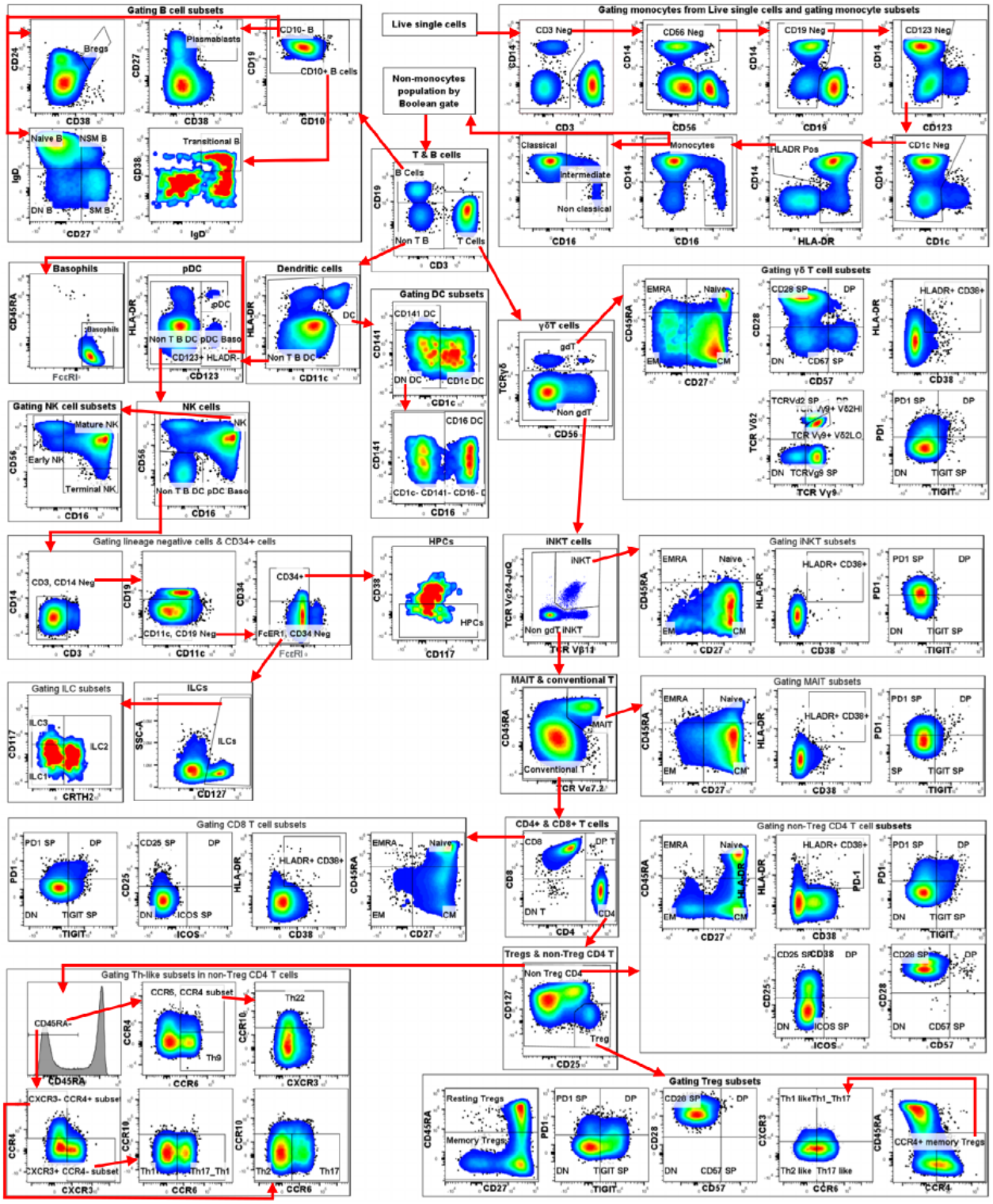

FIGURE 1 Manual gating strategy for the identification of 131 immune subsets from PBMCs. Live, single cells from seven technical replicates were concatenated to a single FCS file before gating. Bregs, regulatory B cells; CM, central memory; DC, dendritic cells; DP, double positive; EM, effector memory; EMRA, effector memory re-expressing RA; ILC, innate lymphoid cells; Neg, negative; Pos, positive; Tregs, regulatory T cells; pDC, plasmacytoid dendritic cells; SP, single positive

minus one (FMO) control. Monocytes were initially gated from the live, single cells in a multiple step gating sequence to enable the selection of CD14 dim monocytes. Overlay of manually gated monocytes and fluorescence intensities of CD14 and CD16 on opt-SNE plot showed that the gating does not include other cell types (Figure S1 (B)). Due to the use of serial gating to define monocytes, non-monocyte population was created by a Boolean gate excluding the monocyte population from live single cells. Other immune subsets

were gated from this nonmonocyte population. As our study used healthy donor PBMCs only, ICOS and LAG-3 did not have a significant number of positive events. The manual gating shows that all other immune subsets were resolved in a satisfactory manner. Even though, the panel used fluorochromes with very similar emission spectra, the positive populations have satisfactory resolution when compared to single stained cells (Figure S2).

Heatmap overlay of all the 43 fluorochromes as well as autofluorescence (AF) of the cells extracted by SpectroFlo software on opt-SNE plot is shown in Figure S3. All the individual seven technical replicates were overlaid on opt-SNE plot (Figure S1(C)). The figure shows that all the clusters contain a similar proportion of each sample that indicates reproducible staining. The major immune subsets obtained by manual gating were overlaid on opt-SNE and UMAP dimensionality reduction plots (Figure S1(D)) and all the subsets formed well defined clusters on both DR plots. The opt-SNE and UMAP plots show that the dimensionality reduction visualizations were able to separate relatively minor populations such as DC and ILC, but their subsets (e.g., CD141+ DCs, CD1c+ DCs, CD16+ DCs, ILC1, ILC2, ILC3) cannot be resolved into separate clusters. If identification of rare subsets is of importance manual gating by an expert is the best choice, although it requires more effort and hands-on time. FlowSOM is one of the few clustering algorithms that allows to provide expected number of clusters while other clustering algorithms like Phenograph identify number of clusters based on the K value. Phenograph (detecting only 32 clusters with this data set; data not shown) and FlowSOM (with 45 Meta Clusters) does not identify those smaller subsets (Figure S1(E)). Instead, large immune subsets like CD4+ and CD8+ T cells were divided into smaller clusters. This is one of the limitations of automated algorithms.

Using the uniqueness score of the fluorochrome full spectrum emission signature, the SpectroFlo software calculates a Similarity Index Matrix (SIM), which reflects the fluorochrome combination compatibility. The value 0 indicates the absence of spectral similarity between fluorochromes while value 1 indicates identical spectral signature. Recent publication by Park et al. [2] shows that fluorochrome pairs with similarity index value of 0.98 or less can be accurately unmixed using appropriate single-stained reference controls. Our 43 color panel had a overall Complexity Index of 99.51 (Figure S4(A)), with three fluorochrome pairs (FITC – BB515; PerCP Cy5.5 – BB700; AF700 – APC-R700) with SIM above 0.9 but below 0.98. The panel was designed to avoid co-expressing markers with fluorochrome combinations with higher similarity index, which can reduce the impact on marker resolution. Out of 903 possible combinations, only 56 fluorochrome combinations had a similarity index above 0.5. The staining of three fluorochrome combinations with highest similarity index on all live cells are shown in Figure S4(B).

OMIP-58 [14] and OMIP-44 [15] are highly optimized multicolor panels that utilizes 28–30 parameters to thoroughly phenotype the T cell and dendritic cell compartment within human PBMCs. OMIP-63 [16] is a 27 color panel that enables broad phenotyping of human innate like lymphocytes, conventional T cells and B cells. OMIP-64 [17] was designed to characterize human NK cells, innate lymphoid cells, unconventional, and conventional T cells in the context of immune response toward vaccination using 26 markers. Some of these panels together can characterize almost entire cellular subsets of human PBMCs. But the complexity of running several panels/tubes to characterize entire cellular subsets would require more sample and some data is lost as the marker expression details comes from different staining tubes. OMIP-69 enables in-depth characterization of human PBMCs including monocytes, basophils. NK cells, dendritic cells, innate lymphoid cells, B cells, and T cells (CD4, CD8, and γδ T) using a 40 color panel that utilizes the capabilities of spectral flow cytometry. Our 43 color panels further pushes the limits of this technology to enable the use of three more additional markers to include more subsets of unconventional T cells and hematopoietic progenitor cells. This panel shares several markers with the 28-color conventional T cell, unconventional T cells and NK cells specific OMIP-58, and the 28-color human dendritic cell compartment specific OMIP-44. Also, the panel includes selected markers from both OMIPs and few B-cell specific markers from OMIP-47 [18] to enable identification of monocytes and their subsets, B cells and their subsets, dendritic cells and their subsets, and plasmacytoid dendritic cells along with conventional and unconventional T-cell subsets. The addition of cytokine receptors from OMIP-17 [8] enables the identification of Th-like subsets within the non-Treg $CD4^+$ T cells and Treg populations. Additional markers in our panel enables the identification of innate lymphoid cells and their subsets, hematopoietic progenitor cells and basophils. Although our panel was optimized to stain 1 million PBMCs, the use of laminar wash technology enabled us to stain as low as 2.5×10^5 cells and obtain similar data (data not shown). This panel covers most of the immune subsets within the peripheral immune system that will be helpful to make comprehensive understanding of immune system, especially with low-quantity specimen obtained from patients. The limitation of this work includes the lack of benchmarking of cellular subsets and validations. This work aims to showcase that this panel opens up a possibility to use fluorochrome-based methodology for extremely high-dimensional flow cytometry. The panel can serve as a guide to understand fluorochrome-marker combinations that can work in spectral flow cytometry and can lead the way toward the development of an optimized multicolor immunophenotyping panel.

ACKNOWLEDGMENTS

The authors would like to thank Medical Research Centre, Hamad Medical Corporation for the funding (IRGC-03-NI-17-071 to Kodappully Sivaraman Siveen; IRGC-04-SI-17-151 and MRC-03-19-039 to Martin Steinhoff) and Dr. Michal Kulinski and Dr. Majid Alam for their support. The publication of this article was funded by the Qatar National Library, Doha, Qatar.

AUTHOR CONTRIBUTIONS

Fairooz Sahir: Formal analysis; investigation; project administration. **Jericha Mateo:** Investigation; project administration; resources. **Martin Steinhoff:** Funding acquisition; resources; writing-review and editing. **Kodappully Sivaraman Siveen:** Conceptualization; data curation; formal analysis; investigation; methodology; project administration; software; supervision; visualization; writing-original draft.

CONFLICT OF INTEREST

The authors declare that there are no conflicts of interest.

ORCID

Kodappully Sivaraman Siveen https://orcid.org/0000-0003-4669-1890

REFERENCES

1. Rodriguez L, Pekkarinen PT, Lakshmikanth T, Tan Z, Consiglio CR, Pou C, et al. Systems-level Immunomonitoring from acute to recovery phase of severe COVID-19. *Cell Rep Med*. 2020;*1*(5):100078.
2. Park LM, Lannigan J, Jaimes MC. OMIP-069: forty-color full Spectrum flow cytometry panel for deep Immunophenotyping of major cell subsets in human peripheral blood. *Cytom A*. 2020;*97*(10):1044–1051.
3. Monaco G, Chen H, Poidinger M, Chen J, de Magalhaes J, Larbi A. flowAI: automatic and interactive anomaly discerning tools for flow cytometry data. *Bioinformatics*. 2016;*32*(16):2473–2480.
4. McInnes L, Healy J, Melville J. UMAP: uniform manifold approximation and projection for dimension reduction. *arXiv*. 2018;*1802*:03426.
5. Belkina AC, Ciccolella CO, Anno R, Halpert R, Spidlen J, Snyder-Cappione JE. Automated optimized parameters for T-distributed stochastic neighbor embedding improve visualization and analysis of large datasets. *Nat Commun*. 2019;*10*:5415.
6. Van Gassen S, Callebaut B, Van Helden MJ, Lambrecht BN, Demeester P, Dhaene T, et al. FlowSOM: using self-organizing maps for visualization and interpretation of cytometry data. *Cytom A*. 2015;*87*(7):636–645.
7. Shikuma CM, Chow DC, Gangcuangco LMA, Zhang G, Keating SM, Norris PJ, et al. Monocytes expand with immune dysregulation and is associated with insulin resistance in older individuals with chronic HIV. *PLoS One*. 2014;*9*(2):e90330.
8. Mahnke YD, Beddall MH, Roederer M. OMIP-017: human CD4+ helper T-cell subsets including follicular helper cells. *Cytom A*. 2013;*83A*:439–440.
9. Halim L, Romano M, McGregor R, Correa I, Pavlidis P, Grageda N, et al. An atlas of human regulatory T helper-like cells reveals features of Th2-like Tregs that support a tumorigenic environment. *Cell Rep*. 2017;*20*:757–770.
10. Moura RA, Quaresma C, Vieira AR, Gonçalves MJ, Polido-Pereira J, Romão VC, et al. B-cell phenotype and IgD-CD27- memory B cells are affected by TNF-inhibitors and tocilizumab treatment in rheumatoid arthritis. *PLoS One*. 2017;*12*(9):e0182927.
11. Zaimoku Y, Patel BA, Kajigaya S, Feng X, Alemu L, Quinones Raffo D, et al. Deficit of circulating CD19+ CD24hi CD38hi regulatory B cells in severe aplastic anaemia. *Br J Haematol*. 2020;*190*(4):610–617.
12. Rhodes JW, Tong O, Harman AN, Turville SG. Human dendritic cell subsets, ontogeny, and impact on HIV infection. *Front Immunol*. 2019;*10*:1088.
13. Trabanelli S, Gomez-Cadena A, Salomé B, Michaud K, Mavilio D, Landis BN, et al. Human innate lymphoid cells (ILCs): toward a uniform immune-phenotyping. *Cytom B*. 2018;*94*(3):392–399.
14. Liechti T, Roederer M. OMIP-058: 30-parameter flow cytometry panel to characterize iNKT, NK unconventional and conventional T cells. *Cytom A*. 2019;*95*(9):946–951.
15. Mair F, Prlic M. OMIP-044:28-color immunophenotyping of the human dendritic cell compartment. *Cytom A*. 2018;*93*(4):402–405.
16. Payne K, Li W, Salomon R, Ma CS. OMIP-063: 28-color flow cytometry panel for broad human immunophenotyping. *Cytom A*. 2020;*97*(8):777–781.
17. Hertoghs N, Schwedhelm KV, Stuart KD, McElrath MJ, De Rosa SC. OMIP-064: a 27-color flow cytometry panel to detect and characterize human NK cells and other innate lymphoid cell subsets, MAIT cells, and γδ T cells. *Cytom A*. 2020;*97*(10):1019–1023.
18. Liechti T, Günthard HF, Trkola A. OMIP-047: high-dimensional phenotypic characterization of B cells. *Cytom A*. 2018;*93*(6):592–596.

SUPPORTING INFORMATION

Additional supporting information may be found online in the Supporting Information section at the end of this article.

How to cite this article: Sahir F, Mateo JM, Steinhoff M, Siveen KS. Development of a 43 color panel for the characterization of conventional and unconventional T-cell subsets, B cells, NK cells, monocytes, dendritic cells, and innate lymphoid cells using spectral flow cytometry. *Cytometry*. 2020;1–7. https://doi.org/10.1002/cyto.a.24288